Please do not adjust margins

ARTICLE

Bimetallic Scorpionate-based Helical Organoaluminums for the Efficient Carbon Dioxide Fixation into a Variety of Cyclic Carbonates

Received 00th January 20xx,
Accepted 00th January 20xx

DOI: 10.1039/d0cy00593b

Marta Navarro,[a] Luis F. Sánchez-Barba,*[a] Andrés Garcés,*[a] Juan Fernández-Baeza,[b] Israel Fernández,*[c] Agustín Lara-Sánchez,[b] and Ana M. Rodríguez[b],

A new family of bimetallic helical aluminum complexes can be obtained via warming up the preliminary dinuclear adduct complexes, or alternatively, by direct heating of the protioligands with 2 equiv of AlR_3. X-ray diffraction analysis corroborated both high coordination versatility in the ligands and the existence of helical chirality in the complexes. DFT calculations confirmed the preferential arrangement of the ancillary scorpionates in the bimetallic complexes and rationalized a proposed reaction mechanism. Bimetallic complexes were investigated as catalysts in combination with halides for the cycloaddition reaction of CO_2 with a wide range of epoxides for cyclic carbonate formation. These studies led to the development of a sustainable, inexpensive, efficient and selective bicomponent system with very broad substrate scope, including internal and challenging bio-based trisubstituted terpene derived substrates, reaching high conversions for *trans*-limonene oxide at mild conditions (79% conv., 70 ºC, 10 bar CO_2, 1 mol%, 66 h).

Introduction

The indiscriminate use of our natural resources is having an incredible impact on sustainability of our planet. The transition from the current linear to a circular model of economy provides an efficient waste management and represents one of the most important challenges in this century.[1] Within this new paradigm, exploitation of long-lived greenhouse gases, such as CO_2, provides a substantial economic growth along with the benefits of mitigating climate change impact. Therefore, chemical utilization of CO_2 as C1 resource for the production of valuable chemicals has attracted much attention during the last two decades,[2] since CO_2 represents a renewable, non-toxic, abundant and inexpensive molecule. In particular, one of the most studied processes for CO_2 valorisation is the 100% atom-economical synthesis of cyclic carbonates (CC's) by cycloaddition of CO_2 to epoxides (see Scheme 1).

CC's are highly demanded products due to their multiple applications in chemical industry,[3-9] such as solvents for Li-ion batteries, greener polar aprotic solvents and raw material for engineering plastics. In addition, the coupling reaction of CO_2 and epoxides represents an emerging methodology to the traditional and toxic reaction of 1,3-diols and phosgene derivatives.[10] For this reason, effective catalysts have been developed to promote this reaction under milder conditions, including heterogeneous[11] and homogenous catalysts.[12] The use of organocatalysts is well established for both approaches,[13] although metal-based catalysts are by far the most common species employed.

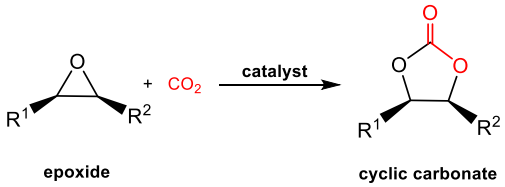

Scheme 1. Synthesis of cyclic carbonates.

Particularly, over the last years efficient one- and bicomponent catalytic systems have been reported for the synthesis of CC's by the coupling reaction of CO_2 with epoxides. For instance, complexes based on chromium,[14] cobalt,[15] iron,[16] magnesium,[17] zinc,[18] or aluminum,[19] have successfully catalysed this reaction. Nonetheless, there is still a demand for the development of sustainable catalysts that display higher activity under milder reaction conditions for challenging epoxides such as internal and bio-based derived substrates. Interestingly, the fact that aluminum is the most abundant metal present in the Earth's crust, along with its low environmental impact and high catalytic activity makes it particularly attractive for its application to CC's synthesis.

On the other hand, catalytic performance is highly dependent on the auxiliary ligand of the complex. In this sense, over the last few

Published article available at
https://pubs.rsc.org/en/content/articlelanding/2020/cy/d0cy00593b#!divAbstract

[a] *Departamento de Biología y Geología, Física y Química Inorgánica. Universidad Rey Juan Carlos. Móstoles-28933-Madrid, Spain. E-mail: luisfernando.sanchezbarba@urjc.es andres.garces@urjc.es*
[b] *Departamento de Química Inorgánica, Orgánica y Bioquímica-Centro de Innovación en Química Avanzada (ORFEO-CINQA). Universidad de Castilla-La Mancha. Campus Universitario, 13071-Ciudad Real, Spain*
[c] *Departamento de Química Orgánica I and Centro de Innovación en Química Avanzada (ORFEO-CINQA). Facultad de Ciencias Químicas, Universidad Complutense de Madrid. 28040, Madrid, Spain. E-mail: israel@quim.ucm.es*

† Dedicated to Professor Antonio Otero on the occasion of his retirement.

Electronic Supplementary Information (ESI) available: Spectroscopic details of complexes **1**-**9**, X-ray diffraction studies for complexes **1**, **3**, **4**, **6** and **8**, selective ^{1}D NOESY experiments, experimental details for the synthesis of cyclic carbonates, including ^{1}H and ^{13}C NMR spectra of cyclic carbonates **11a-j**, **13a-f** and **15**, kinetic studies, and DFT experimental computational details. CCDC 1992424-1992428. For ESI and crystallographic data in CIF or other electronic format See DOI: 10.1039/x0xx00000x

Please do not adjust margins

Please do not adjust margins

years our research group has developed a wide variety of catalytic species supported by scorpionate ligands, which are among the most versatile and tuneable ancillaries employed to stabilize a wide range of active complexes for high-tech catalytic processes.[20] Therefore, we have reported highly active one- and bicomponent aluminum catalysts stabilized by NNO- and NNS-scorpionate ligands[21] as environmental friendly and efficient catalysts for CO_2 cycloaddition to epoxides.

With the stimulating aim to design sustainable and more efficient catalysts for this demanding process, we now focus on exploring the catalytic behaviour of new dinuclear aluminum complexes supported by amidinate-based scorpionate ligands, where cooperation between centres might add benefit to their catalytic performance.[22] For this propose, we take advantage on the high versatility that our amidinate-based scorpionates offer in their coordination modes in the form of two possible tautomers, as a result of the two acidic protons (Chart 1,*a*).[23] This has been subsequently verified through the preparation of mononuclear aluminun-based complexes supported by these scorpionates, in the form of CH and NH tautomers, which resulted efficient initiators for the living and immortal ring-opening polymerization of cyclic esters (Chart 1,*b*).[23] Considering these scorpionate features, we have also designed helical aluminum complexes that not only can act as building blocks for the construction of metallic helicates[24] as promising entities in medicinal chemistry or asymmetric catalysis,[25] but also displayed high catalytic activity for carbon dioxide fixation into cyclic carbonates.[26]

We report hereby the preparation of a new family of bimetallic helical aluminum complexes supported by amidinate-based scorpionates as catalysts for CO_2 fixation into five-membered cyclic carbonate products. These bimetallic species exhibit excellent performance through an intramolecular cooperative mechanism, and display very broad substrate scope, including internal and challenging bio-based derivatives such as limonene oxide.

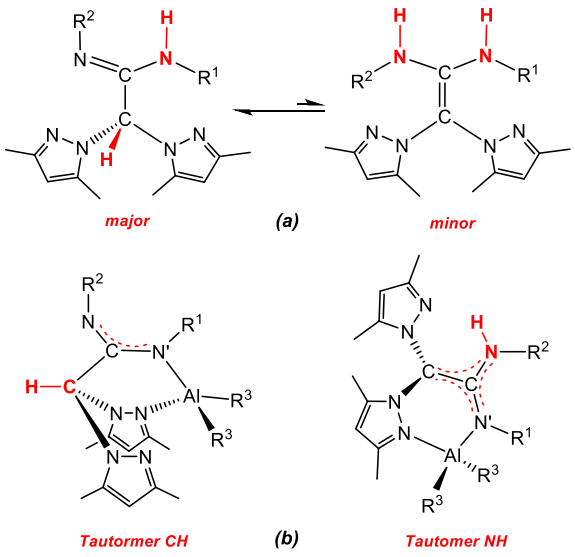

Chart 1. (*a*) Possible tautomers of the amidinate-based scorpionate ligands, (*b*) versatility in the coordination modes found in the corresponding mononuclear helical aluminum-based complexes.

Results and Discussion

Synthesis and Characterization of Complexes

We initially reacted the mononuclear scorpionates [$AlMe_2$(κ^2-*NN*'](κ^2-*NN*' = pbpamd **1**; tbpamd[23]), as only NH tautomers, with one equivalent of the commercially available $AlMe_3$ in toluene at 20 ºC to afford the Lewis acid-base adduct helical complexes [$AlMe_2$(κ^2-*NN*'-κ^1-*N*)$AlMe_3$] (**2**–**3**) (κ^2-*NN*'-κ^1-*N* = pbpamd, **2**; tbpamd, **3**) (see Scheme 2*b*). This reaction did not progress in tetrahydrofuran. The precursor helical complex [$AlMe_2$(κ^2-pbpamd)] (**1**) was prepared accordingly to our earlier work,[23] employing the scorpionate protioligand, Hpbpamd (Hpbpamd = *N,N'*-diisopropyl bis(3,5-dimethylpyrazol-1-yl)acetamidine)[27], with one equiv of $AlMe_3$ also at 20 ºC, but using tetrahydrofuran as solvent in order to produce only the NH tautomer (see Scheme 2*a*). Accordingly, complexes **1**–**3** were obtained in good yields (*ca.* 85%) as white solids after the appropriate work up. It was noteworthy that the direct reaction of the protioligands with 2 equiv of $AlMe_3$ did not work at this temperature in toluene or tetrahydrofuran.

Interestingly, the reaction of the scorpionate protioligands, Hpbpamd,[27] Htbpamd (Htbpamd = *N*-ethyl-*N'*-*tert*-butylbis(3,5-dimethylpyrazol-1-yl)acetamidine),[27] and Hphbpamd (Hphbpamd = *N,N'*-di-*p*-tolylbis(3,5-dimethylpyrazol-1-yl)acetamidine)[28] with two equivalents of AlR_3 in toluene at high temperature cleanly affords the dinuclear amidinate-based scorpionate aluminum complexes [AlR_2(κ^2-*NN'*;κ^2-*NN'*)AlR_2] (κ^2-*NN'*;κ^2-*NN'* = pbpamd$^-$, R = Me **4**, Et **5**; tbpamd$^-$, R = Me **6**, Et **7**; phbpamd$^-$, R = Me **8**, Et **9**) as white or pale yellow solids in excellent yields (*ca.* 90%) (see Scheme 3*a*). Remarkably, the activation process of the N–H and the bridging C–H takes place in all scorpionate ligands, resulting in the formation of an extended π-C_2N_2(sp^2)–Al_2 structure.

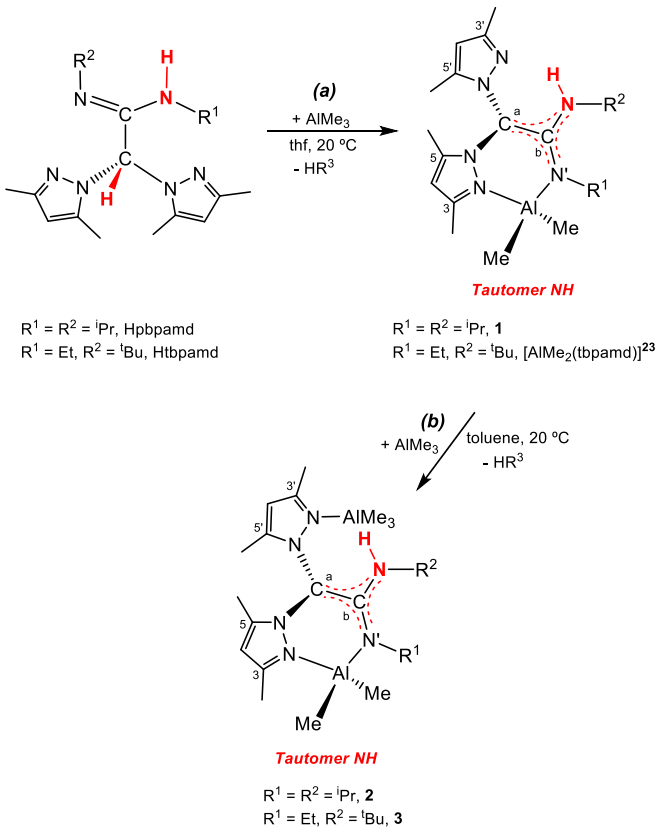

Scheme 2. Synthesis of the helical complexes **1**–**3**.

This journal is © The Royal Society of Chemistry 20xx

Please do not adjust margins

Please do not adjust margins

Alternatively, when a toluene solution of the adduct complexes (*i.e.*; **2** or **3**) is warmed up, the corresponding bimetallic complexes (**4** or **6**) are obtained in a quantitative yield (see Scheme 3*b*).

The ^{1}H and ^{13}C-{^{1}H} NMR spectra of complexes **1**–**3** in benzene-d_6 at room temperature (see Figure S1-S3 in the Electronic Supplementary Information) present the characteristic signal for the N−H group and two sets of resonances for the inequivalent pyrazole rings. The amidinate fragment also shows two set of signals, in agreement with a monodentate binding mode. Interestingly, a new signal appears at high fields corresponding to the additional $AlMe_3$ in complexes **2**–**3**. ^{1}H NOESY-1D experiments confirmed coordination of the $AlMe_3$ to the free pyrazol ring (see Figure S10 in the ESI†).

The solid-state crystal structures of **1** and **3** were confirmed by X-ray diffraction analysis, and showed the proposed κ^2-*N,N'* arrangement for the scorpionate ligand in the NH tautomeric form coordinated to a distorted tetrahedral aluminum centre in both complexes (see Figure S11 for **1** in the ESI† and Figure 1 for **3**). For complex **3**, the ligand tbpamd coordinates to Al(2) through one pyrazole ring, N(1), and the amidinate fragment, N(6) (1.950(3) Å and 1.865(3) Å, respectively). The planar geometry of C(6) and C(12) atoms in the π-HN-C_2-N'(sp^2) fragment and coordination of the second $AlMe_3$ (Al(1)-N(3), 2.051(3) Å) were also established. Furthermore, the restricted rotation around the C^a–C^b bond leads to an inherent helical chirality.[29] As a consequence, **1** and **3** crystallize as racemates (*i.e.* an equimolecular mixture of *M* and *P* enantiomers in the unit cell). (see Table S1 and Table S2 in the ESI† for selected bond lengths and angles, and crystallographic details, respectively).

In addition, the ^{1}H NMR spectra in benzene-d_6 of complexes **4**–**9** at room temperature are consistent with the proposed arrangement (see Figures S4-S9 in the ESI†). Thus, there is only one set of resonances for the Me[3,5] and H[4] in the pyrazole rings and the amidinate fragment, when the amidinate substituents are identical (**4**–**5** and **8**–**9**), according to their symmetric nature (see Scheme 3). Two additional signals at high fields are observed for the non-equivalent alkyl groups bound to the aluminum atoms. In contrast, the spectra for **6** and **7** with different amidinate fragment substituents, show two set of resonances for the inequivalent

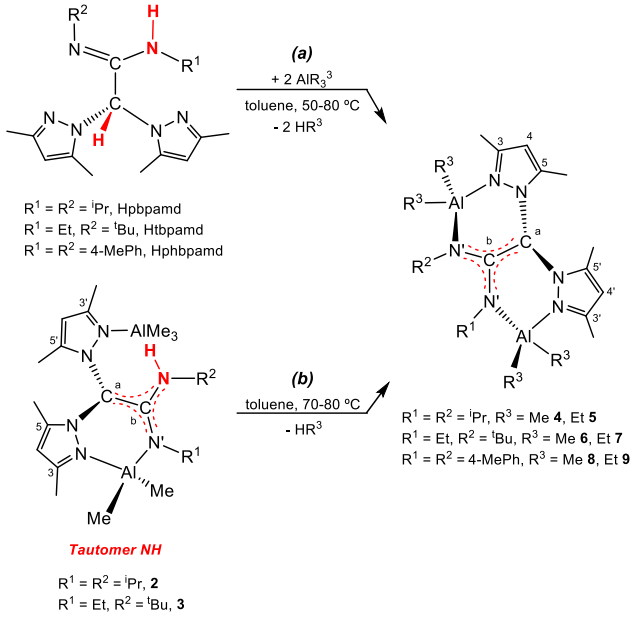

Scheme 3. Synthesis of the dinuclear helical complexes **4**–**9**.

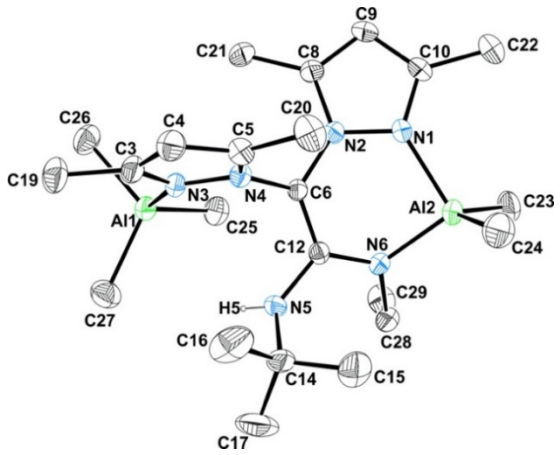

Figure 1. ORTEP view of the *M*-enantiomer of [$AlMe_2$(κ^2-tbpamd)$AlMe_3$] (**3**). Hydrogen atoms have been omitted for clarity. Thermal ellipsoids are drawn at the 30% probability level. Distances (Å): Al(1)-N(3) = 2.051(3); Al(2)-N(1) = 1.950(3); Al(2)-N(6) = 1.865(3); N(2)-C(6) = 1.431(4); N(5)-C(12) = 1.401(4); C(12)-N(6) = 1.360(4); C(12)-C(6) = 1.369(5). Angles (º): C(25)-Al(1)-N(3) = 111.20(17); N(6)-Al(2)-N(1) = 94.29(13); C(12)-C(6)-N(4) = 122.4(3); C(12)-C(6)-N(2)= 123.7(3); N(4)-C(6)-N(2) = 113.0(3); N(6)-C(12)-C(6) = 121.4(3); N(6)-C(12)-N(5) = 120.1(3); C(6)-C(12)-N(5) = 118.5(3).

pyrazole rings, and four signals at negative shift for the alkyl groups bound to the metals.

X-ray diffraction studies for complexes **4**, **6** and **8** confirm a monomeric dinuclear structure for all complexes (see Figure 2 for **4**, and Figures S12 and S13 in the ESI† for **6** and **8**, respectively). Selected bond lengths and angles are collected in Table S3 for **4**, **6** and **8**, and crystallographic details are reported in Table S4. In all cases, the aluminum centres present a distorted tetrahedral geometry and are bridged by one single scorpionate ligand, which is in a κ^2-*N,N'*;κ^2-*N,N'* coordination mode occupying two positions of each metal.

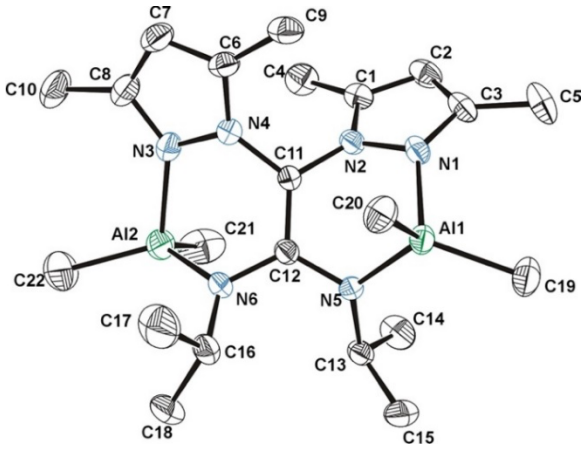

Figure 2. ORTEP view of the *M*-enantiomer of [$AlMe_2$(pbpamd$^-$)$AlMe_2$] (**4**). Hydrogen atoms have been omitted for clarity. Thermal ellipsoids are drawn at the 30% probability level. Distances (Å): Al(1)-N(1)= 1.977(2); Al(2)-N(3)= 1.971(2); Al(1)-N(5)= 1.866(2); Al(2)-N(6)= 1.871(2); N(5)-C(12)= 1.376(2); N(6)-C(12)= 1.379(2); C(11)-C(12)= 1.378(2). Angles (º): N(5)-Al(1)-N(1)= 94.62(7); N(6)-Al(2)-N(3)= 95.36(7); C(12)-N(5)-Al(1)= 113.9(1); C(12)-N(6)-Al(2)= 114.8(1); C(12)-C(11)-N(4)= 123.9(2); C(12)-C(11)-N(2)= 122.8(2); N(4)-C(11)-N(2)= 113.3(1); N(5)-C(12)-N(6)= 123.7(2).

Please do not adjust margins

Please do not adjust margins

The Al-N(pyrazole) distances (1.959(5)-2.002(4) Å) are slightly longer than the Al-N'(amidinate moiety) (1.866(2)-1.888(4) Å), whilst Al-C distances (1.935(6)-2.009(6) Å) are similar to those previously reported.[21e,23,30] More interestingly, the planar π-extended C_2–N_2 system is evidenced by both angles close to 120º around C^a and C^b atoms and the C(11)–C(12) bond lengths [1.377(7)–1.378(2) Å] between C–C single (~1.455 Å) and double (~1.339 Å) bond. As in the case of **1** and **3**, an equimolecular mixture of *M* and *P* enantiomers is present in the unit cell (see Figures S14a and S14b in the ESI†, *i.e.* for **6**).

Density Functional Theoretical Calculations

Density Functional Theory (DFT) calculations at the dispersion corrected PCM(toluene)–B3LYP-D3/6-31G* level (see computational details in the ESI†) were carried out to study the thermodynamic stability of the three families of complexes described above, named the mononuclear **1** and the analogous [$AlMe_2$(κ^2-tbpamd)][23] and [$AlMe_2$(κ^2-phbpamd)],[23] the dinuclear adducts **2**–**3** (see Scheme 2) and the bimetallics **4**–**9** (see Scheme 3), in order to (*i*) rationalize the particular arrangement observed for the scorpionate ligands in the bimetallic aluminum complexes **4**–**9**, and (*ii*) propose a plausible mechanism through which, these complexes can be obtained.

We initially inspected the different thermodynamic stability of the two possible coordination modes for these dianionic scorpionate ligands, namely (*a*) apical carbanion σ-C(sp^3)-Al *versus* (*b*) extended planar π-C_2N_2(sp^2)–Al_2, (see Figure 3) previously observed for analogous magnesium alkyls.[28] Complexes **4** and **8**, were selected as they show the greater disparity regarding their electronic and steric features (*i.e.* pbpamd$^-$ for **4** and phbpamd$^-$ for **8**). The planar π-C_2N_2 structure (*b*) was found to be much more stable for both complexes **4** and **8**, lying 25.9 kcal/mol and 18.6 kcal/mol, respectively, below the corresponding apical species, which was fully consistent with the exclusive π-C_2N_2(sp^2)–Al_2 arrangement experimentally found for complexes **4**–**9**.

Then, we focused on the formation of complexes **4**, **6** and **8** from the reaction of species **1**, [$AlMe_2$(κ^2-tbpamd)][23] and [$AlMe_2$(κ^2-phbpamd)][23] with $AlMe_3$ (see Figure 4). Coordination of the free pyrazole nitrogen atom of these complexes to $AlMe_3$ affords complexes **2**–**3**, and a not isolated analogous adduct [$AlMe_2$(κ^2-phbpamd)$AlMe_3$] in a strongly exergonic process (ΔG_R = -8.4 to -15.7 kcal/mol).

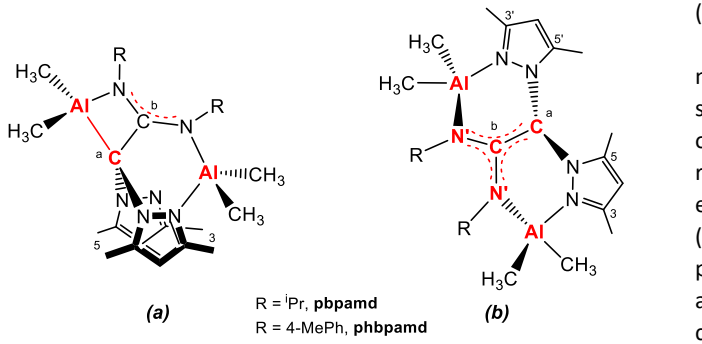

Figure 3. Possible coordination modes for the acetamidinate scorpionate ligands pbpamd$^-$ and tbpamd$^-$: (*a*) apical carbanion with direct σ-C(sp^3)–Al covalent bond and (*b*) extended planar π-C_2N_2(sp^2)–Al_2 covalent bond.

These intermediate adducts evolve into complexes **4**, **6** and **8** therefore releasing a molecule of CH_4 via the corresponding transition state **TS** in a highly exergonic transformation (ΔG_R = -38.7 to -48.5 kcal/mol, calculated from the isolated initial reactants). This saddle point is associated with the migration of the hydrogen atom of the N–H moiety to one of the methyl substituents of the coordinated $AlMe_3$ with the concomitant Al–C bond rupture and formation of a new N–Al bond. Interestingly, the computed activation barriers $\Delta G^{\neq}$ = 37.4 kcal/mol (**1**), 38.0 kcal/mol ([$AlMe_2$(κ^2-tbpamd)])[23], 28.3 kcal/mol ([$AlMe_2$(κ^2-pbpamd)])[23] are consistent with the milder reaction conditions required for the formation of complex **8** as compared to **4** or **6** (see Scheme 3).

Catalytic Studies for the Cycloaddition of CO_2 to Epoxides for Cyclic Carbonates Production

Catalysts Screening

Initially, representative mononuclear, adduct and dinuclear aluminum complexes, namely **1**, **2**–**3**, and **4**, **6** and **8**, respectively, were tested as catalysts for the formation of styrene carbonate **11a** by the coupling reaction of CO_2 with styrene oxide **10a** as a benchmark reaction (see Scheme 4). The process was assessed at 25 ºC, 1 bar of CO_2 pressure and under solvent free conditions for 3, 6 and 18 hours in a 1:1 molar ratio for the methylaluminum complexes selected and in the presence of tetrabutylammonium bromide (TBAB), which was used as representative co-catalyst, using a catalyst loading of 5%. The results are presented in Table 1. Styrene oxide conversion into the styrene carbonate was determined by ^{1}H NMR at the established time intervals without any further purification (see Figure S15 in the ESI†). Formation of polycarbonate was not detected under the aforementioned conditions (selectivity >99%).

All dinuclear aluminum complexes, including tetraalkyls **4**, **6**, and **8** (Table 1, entries 4–6), and adduct precursors **2** and **3** (Table 1, entries 2 and 3) displayed much higher catalytic activity than the mononuclear counterpart **1** (Table 1, entry 1) for the synthesis of **11a**. However, it should be noted that these dinuclear aluminum complexes benefit from the presence of an additional aluminum centre (10 mol%) under these conditions. Therefore, to investigate the role of both aluminum centres in the process, *i.e.* whether they function separately or in a cooperative manner, additional experiments were carried out for the conversion of **10a** into **11a** employing the more active complex of both dinuclear families (complex **4**).

Firstly, we explored the effect of using different catalyst/TBAB molar ratios, maintaining the rest of conditions unaltered. In this sense, when the coupling reaction was conducted employing a 2.5% of catalyst **4** loading and 5% of TBAB (Table 1, entry 11), only a slight rise in the conversion was observed after 18 h compared with the experiment conserving a 2.5% loading for both catalyst and TBAB (Table 1, entry 10) (48% *vs* 42%). This small increase is not enough to postulate that both centres act independently, and it can be attributed to the small contribution of TBAB excess. Additionally, the cooperative features of **4** can be also elucidated by comparing its performance with the corresponding monometallic counterpart **1**, but maintaining in both cases identical metal concentration.

This journal is © The Royal Society of Chemistry 20xx

Please do not adjust margins

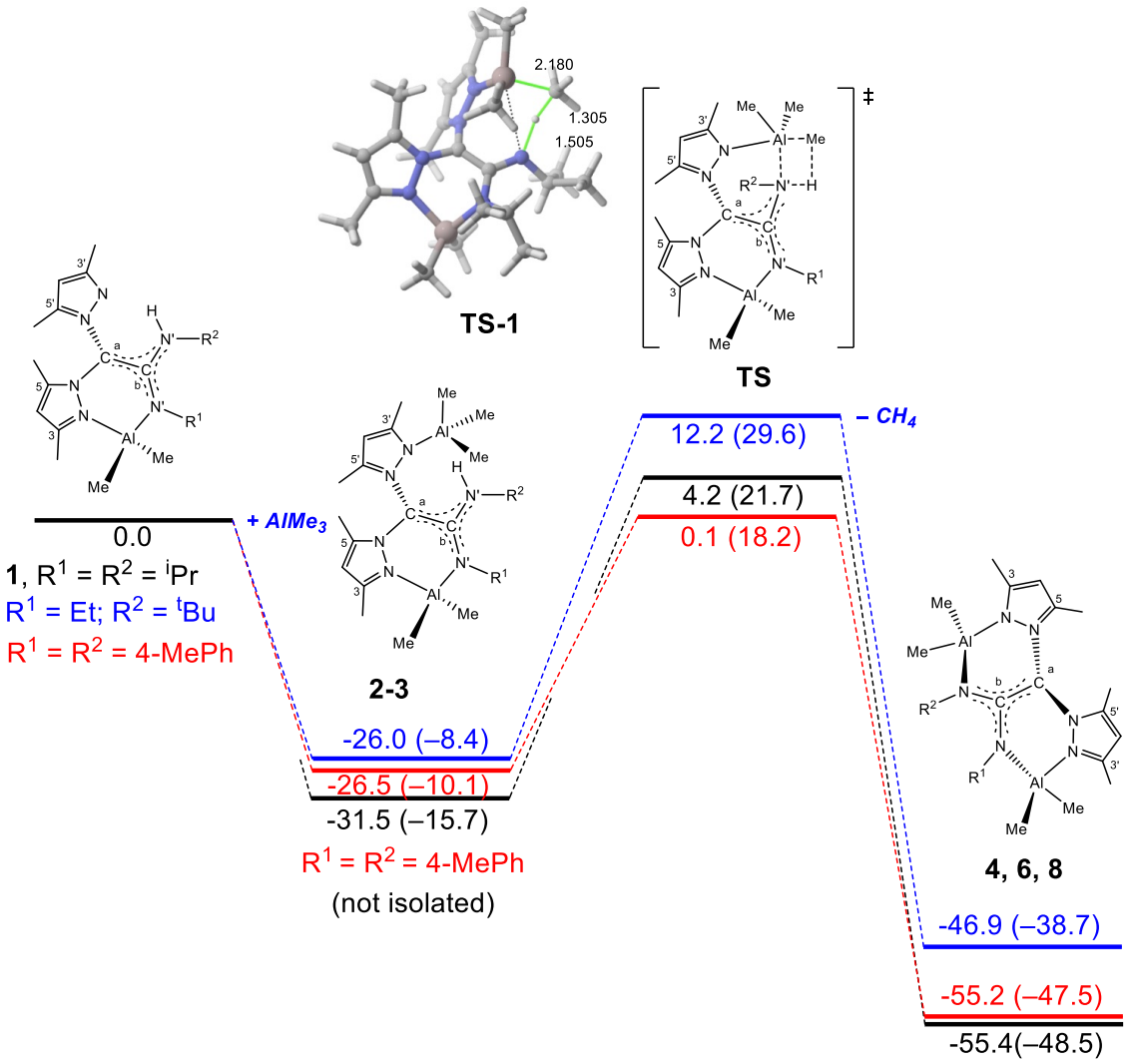

Figure 4. Computed reaction profiles for the formation of the extended planar π-C_2N_2 dinuclear aluminum scorpionates **4**, **6** and **8**. Relative energies (free energies, ΔG, at 298 K, are given within parentheses) and bond distances are given in kcal/mol and angstroms, respectively. All data have been computed at the PCM(toluene)–B3LYP-D3/6-31G(d) level.

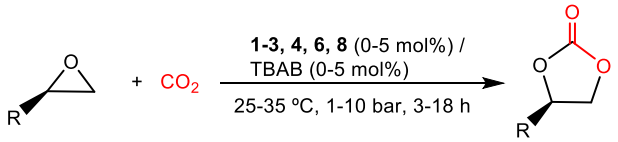

a: R = Ph; **b**: R = C_4H_9; **c**: R = C_8H_{17}; **d**: R = $C_{10}H_{21}$; **e**: R= CH_2Cl
f: R = CH_2OH; **g**: R = $PhOCH_2$; **h**: R =$C_3H_5OCH_2$; **i**: R = 4-BrC_6H_4
j: R = $(CH_2OCH_2CH_2)_2$

Scheme 4. Cyclic carbonate synthesis catalysed by aluminum scorpionate complexes **1**–**3**, **4**, **6** and **8**.

Indeed, whereas a 2.5 mol% loading of **4** converts 42% of epoxide **10a** (Table 1, entry 10) at 25 °C and 1 bar CO_2 pressure, only 25% conversion was observed for **1**, even though when a double catalyst loading (5%) is used for **1** (Table 1, entry 1), in addition to the beneficial 2.5 mol% of extra co-catalyst. This behaviour supports the hypothesis of a collaborative performance between both aluminum centres in complex **4** for the catalytic reaction. In order to definitively corroborate this observation, kinetics investigations confirmed apparent first-order dependence on the catalyst and co-catalyst concentrations,[31] (see full study in Figures S33 and S34 and Table S5 in the ESI†), which supports an intramolecular cooperative bimetallic mechanism. Furthermore, a control experiment for **4** in the absence of TBAB revealed no catalytic activity, whilst using TBAB with no presence of **4** yielded minimal conversion (4%) after 18 h (Table 1, entries 7 and 8, respectively). In addition, the performance of the corresponding protioligand in complex **4** in the presence of TBAB was also examined, showing no significant conversion (5%) under these conditions (Table 1, entry 9).

Moreover, we decided to explore the effect of temperature and pressure for the synthesis of **11a** from **10a** using complex **4** as a catalyst, by working at 50 °C and 10 bar CO_2 pressure. Interestingly, under these conditions, catalyst and co-catalyst loading can be reduced at 0.5 mol% to achieve almost complete conversion in only 6 hours (Table 1, entry 12), therefore showing better performance than either bimetallic amidate-[22a] or thioacetamidate-[21f-g] based scorpionate organoaluminums previously reported. Expectedly,

Please do not adjust margins

Table 1. Conversion of epoxide **10a** into styrene carbonate **11a** using selected catalysts[a]

Entry	Catalyst	[Cat]:[co-cat] [mol%]	T. [ºC]	Conversion [%] 3 h[b]	6 h[b]	18 h[b]
1	**1**	5.0:5.0	25	11	18	25
2	**2**	5.0:5.0	25	19	30	59
3	**3**	5.0:5.0	25	17	27	57
4	**4**	5.0:5.0	25	23	35	64
5	**6**	5.0:5.0	25	15	28	54
6	**8**	5.0:5.0	25	16	31	56
7	**4**	5.0:0	25	0	0	0
8	**TBAB**	0:5.0	25	0	0	4
9	**Hpbpamd**	5.0:5.0	25	0	0	5
10	**4**	2.5:2.5	25	12	24	42
11	**4**	2.5:5.0	25	14	26	48
12	**4**[c]	0.5:0.5	50	47	90	100
13	**4**[c]	0.5:1.0	50	49	92	100
14	**4**[c]	0.25:0.25	80	100	-	-

[a] Reactions carried out at 25 ºC and 1 bar CO_2 pressure using 5 mol% of complexes **1**–**3**, **4**, **6** and **8**/5 mol% of TBAB as co-catalyst unless specified otherwise. [b] Determined by ^{1}H NMR spectroscopy of the crude reaction mixture. [c] Reactions carried out at 10 bar CO_2 pressure.

double co-catalyst loading produced similar conversion, proving intramolecular cooperative functionality between centers (Table 1, entry 13). Thermal stability of catalyst **4** was also successfully assessed (80 ºC), reaching greater activities even at lower catalyst loadings (0.25 mol%) in 3 hours (Table 1, entry 14), in agreement with the thermodynamic stability of this catalyst, rationalized by DFT calculations (see Figure 4). Therefore, according to the results presented in Table 1, complex **4** was chosen as the most efficient catalyst for further investigations under these experimental conditions, employing different co-catalysts and a wide range of terminal, internal and bio-derived, including trisubstituted, epoxides.

Effect of co-catalyst

Regarding the role of the co-catalyst employed, a series of similar experiments were conducted at 25 ºC and 1 bar CO_2 pressure for the synthesis of **11a** from **10a** in the presence of **4** with different nucleophilic sources. Conversion data presented in Table 2 were collected after 18 hours of reaction, showing the best values of activity for the combination **4**/TBAB. Indeed, when TBAB is replaced

Table 2. Studies on the influence of the co-catalyst on the catalytic activity and optimization of the synthesis of styrene carbonate **11a**, using catalyst **4**[a]

Entry	Co-catalyst (mol%)	Conversion [b] (%)
1	**TBAB**	64
2	**TBAC**	38
3	**TBAI**	34
4	**TBAF**	0
5	**DMAP**	0
6	**PPNCl**	0
7	**NMI**	19

[a] Reactions carried out at 25 ºC and 1 bar CO_2 pressure for 18 h using 5 mol% of catalyst **4** and 5 mol% of co-catalyst. [b] Determined by ^{1}H NMR spectroscopy of the crude reaction mixture.

by other tetraalkylammonium salts such as tetra-*n*-butylammonium fluoride (TBAF), tetra-*n*-butylammonium chloride (TBAC) or tetra-*n*-butylammonium iodide (TBAI) under otherwise identical conditions, lower (in the case of TBAC and TBAI) or null (for TBAF) conversions were obtained (Table 2, entries 1-4). Other co-catalysts such as dimethylaminopyridine (DMAP), bis(triphenylphosphine)iminium chloride (PPNCl) and N-methylimidazole (NMI) resulted in poorly active systems (Table 2, entries 5-7). Therefore, TBAB was identified as the most efficient co-catalyst for complex **4** under these reaction conditions.

Substrate screening

The efficiency of the binary catalytic system formed by **4** and TBAB was firstly tested with ten different mono-substituted epoxides, including alkyl, aryl and functionalized substrates, at 1 bar of CO_2 pressure, and 25 ºC-35 ºC of temperature for 18 h (see Scheme 4), with a catalyst:co-catalyst loading of 5 mol% (see Figures S16-24 in the ESI†). As evidenced in Table 3, catalyst **4** exhibits excellent activities with maintenance of selectivity (>99%) for the cycloaddition reaction with 1,2-epoxyhexane, allyl glycidyl ether and ephiclorohydrin, where full conversions were achieved at 25 ºC (Table 3, entries 2, 5 and 8). Therefore, the presence of electron-withdrawing groups, such chlorine in **10e**, does not apparently affect the reaction progress.[32] However, styrene carbonate formation is a more demanding process due to the lower reactivity of the □-carbon of the epoxide.[33] Indeed, in the case of **10a** and **10i** a slight increase of temperature was necessary to achieve full conversion (Table 3, entries 1 and 9). Likewise, for those substrates bearing alcohol or ether functionalities with phenyl or long alkyl chains, an increase up to 35 ºC is needed to achieve complete or very high conversions, respectively (Table 3, entries 6, 7 and 10), similarly to epoxides with long alkyl chains **10c**–**d** (Table 3, entries 3 and 4).

Considering the good results attained by the bicomponent system **4**/TBAB, we explored the possibility to reduce the catalyst loading and time reaction by increasing the reaction temperature and CO_2 pressure up to 50 ºC and 10 bar, respectively, keeping constant the initial 1:1 catalyst/co-catalyst ratio in the absence of solvent.

This journal is © The Royal Society of Chemistry 20xx

Please do not adjust margins

Please do not adjust margins

Table 3. Conversion of epoxides **10a–10j** into cyclic carbonates **11a–11j** using catalyst **4** and TBAB.[a]

Entry	Epoxide	Conversion [b] at 25 °C (%)	Conversion [b] at 35 °C (%)
1	**10a** (R = Ph)	64	100
2	**10b** (R = C_4H_9)	100	
3	**10c** (R = C_8H_{17})	51	100
4	**10d** (R = $C_{10}H_{21}$)	19	55
5	**10e** (R = CH_2Cl)	100	
6	**10f** (R = CH_2OH)	62	100
7	**10g** (R = $PhOCH_2$)	48	80
8	**10h** (R = $C_3H_5OCH_2$)	100	
9	**10i** (R = 4-BrC_6H_4)	55	100
10	**10j** (R = $(CH_2OCH_2CH_2)_2$)	46	76

[a] Reactions carried out at 1 bar CO_2 pressure for 18 h using 5.0 mol% of catalyst **4** and 5.0 mol% of TBAB as co-catalyst. [b] Determined by ^{1}H NMR spectroscopy of the crude reaction mixture.

Remarkably, these conditions allowed a 5- or even 10-fold reduction in catalyst/co-catalyst loading in the epoxides tested, achieving from very good to excellent conversions in only 8 hours (see Figure 5).

The reactivity of the different epoxides assessed **10a–10j** varies in a similar manner to that observed at 20 ºC and 1 bar CO_2 pressure under these conditions. Thus, those substrates bearing long alkyl chains or ether are again comparatively less reactive (**10d**,**g**,**j**) than their epoxide counterparts (**10a–c**,**e–f**,**h–i**), being necessary a slight increase of the catalyst loading to 1.0 mol%.

In view of the high activity exhibited by the bicomponent system **4**/TBAB, we additionally extended the substrate scope for catalyst **4**, and evaluated the conversion of internal and bio-based derived epoxides **12a–12f** into the corresponding cyclic carbonates **13a–13f** (see Figure 6 and Figures S25-S30 in the ESI†). The use of more challenging epoxides for their coupling reaction with CO_2, such as oxetanes (internal epoxides) **12a–b**, is of particular interest owing to their low reactivity and selectivity towards the synthesis of the corresponding cyclic carbonates. However, this transformation has received far less attention than their mono-substituted analogs,[34] and only a few examples employing aluminum-based complexes as catalyst have been successfully reported over the last few years.[19c,f,e,35]

Interestingly, the synthesis of cyclic carbonates **13a–b** from the corresponding oxetanes can be conducted using low loadings (2.0-2.5 mol%) of the binary system **4**/TBAB, in 1:1 proportion under mild and solvent-free conditions (70 °C, 10 bar CO_2 pressure) in 18 hours (see Figure 6), reaching high conversions values, and showing the efficiency of this system. In addition, the reaction proceeds with retention of the epoxide stereochemistry through a double inversion process,[36] which led to the exclusive formation of the *cis*-isomer for both cyclohexene oxide and cyclopentene oxide, with a selectivity

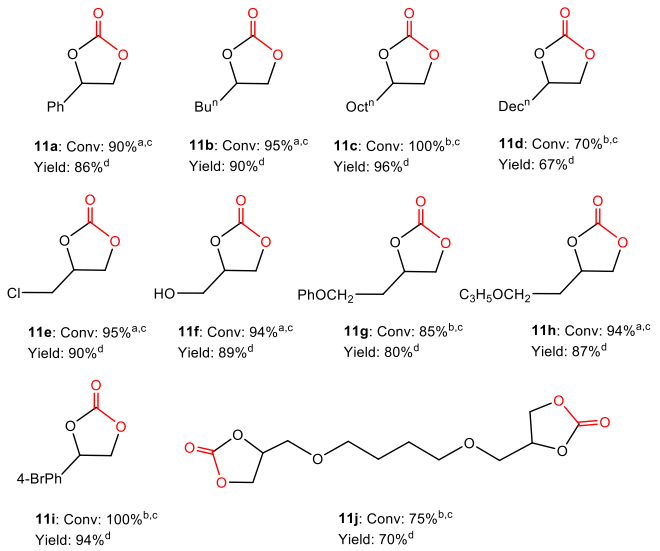

Figure 5. Synthesis of cyclic carbonates **11a–11j** from epoxides **10a–10j** using the system (a) 0.5 mol% or (b) 1.0 mol% of complex **4**/TBAB at 50 ºC and 10 bar CO_2 pressure for 8 hours. (c) Conversion and selectivity were determined by ^{1}H NMR. (d) Isolated yield after column chromatography.

higher than 99%.

Thus, catalyst **4** resulted more efficient for internal epoxides such as **13a** (see Figure 6), than aluminum-based scorpionate catalysts previously reported by our group; *i.e.* very active neutral trimetallic species supported by NN',NO'-donors[21g] (11% conv., 20 ºC, 10 bar, 72 h, 5 mol%), neutral bimetallic NNO-derivatives[21f] (100% conv., 100 ºC, 50 bar, 24 h, 5 mol%), and helical bimetallic NNS-derivatives[21b] (97% conv., 70 ºC, 10 bar, 24 h, 1 mol%, with very low selectivity: 33% PCHC/66% PCHO), or alternative amidinate aluminium complexes,[22a] where no formation of CHC was detected (100% yield to PCHO, 50ºC, 10 bar, 24 h, 7 mol%), or even one-component bimetallic systems bearing chiral NNO-donors[21e] (79% conv., 80ºC, 20 bar, 24 h, 1.5 mol%).[37]

Additionally, we turned our attention to the synthesis of bio-based cyclic carbonates **13c–f** (see Figure 6), since a growing interest has recently emerged toward their potential use as a non-toxic feedstock to produce non-isocyanate poly(hydroxy)urethanes (NIPUs).[38] Therefore, firstly we explored the synthesis of bio-based furan-derived cyclic carbonates, readily accessible from furanyl chemicals, derived from biomass resources such as cellulose.[39] To our delight, excellent conversion was obtained in the synthesis of the bio-based furan-derived cyclic carbonate **13c** after 18 hours at 70 °C and 10 bar CO_2 pressure, employing lower equimolecular catalyst/co-catalyst loading (0.25 mol%) than that used for oxetanes **13a–b**.

This result encouraged us to extend this study to transform other bio-based diepoxides derivatives synthetized from the reaction of glycidol and different acyl dihalide building blocks such as fumaryl, succinil and glutaryl chlorides.[40] We were delighted to find that cyclic carbonates **13d–f** were obtained in quantitative yields under identical conditions than for **13c**, also using only 0.25 mol% of the bicomponent system **4**/TBAB. Thus, catalyst **4** resulted to be similarly efficient as a very active neutral mononuclear NNO-scorpionate aluminum catalyst (**13c–f**: 100% conv., 80ºC, 10 bar CO_2, 3 h, 0.25 mol%),[21a] or bifunctional mononuclear NNO-scorpionate aluminum complexes (**13c–f**: 100% conv., 70ºC, 10 bar CO_2, 18 h, 0.25 mol%),[21d] recently reported.

Please do not adjust margins

Please do not adjust margins

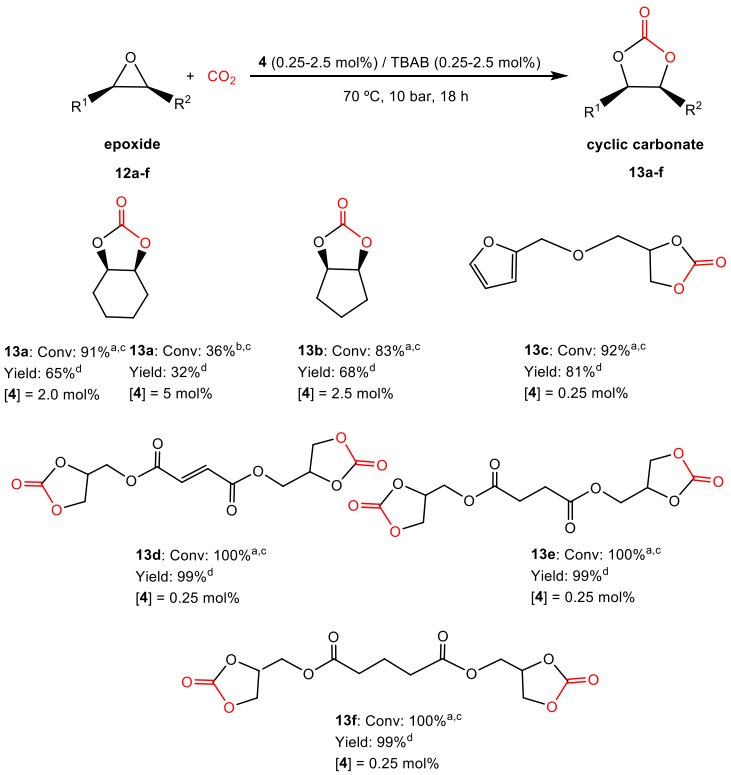

Figure 6. Synthesis of cyclic carbonates **13a**–**13f** from epoxides **12a**–**12f** using equimolecular amounts of the system **4**/TBAB at (a) 70 ºC and 10 bar CO_2 pressure for 18 hours, (b) 20 ºC and 10 bar CO_2 pressure for 72 hours. (c) Conversion and selectivity were determined by ^{1}H NMR. (d) Isolated yield after column chromatography.

More interestingly, another bio-renewable cyclic carbonate that is attracting significant attention is that obtained from limonene, a highly substituted monocyclic unsaturated terpene derived from biomass, mainly extracted from the peel of citrus fruits.[41] However, a very few catalysts have been reported for the successful cycloaddition of CO_2 with limonene oxide (LO).[42,43]

We initially investigated the reaction conditions for the synthesis of the bicyclic limonene carbonate **15** employing the commercially available limonene oxide **14** as a mixture of *cis*/*trans* isomers (43:57) (see Scheme 5, Table 4, and Figure S31 in the ESI†). Thus, we used the bicomponent system formed by complex **4** and bis(triphenylphosphoranylidene)ammonium chloride (PPNCl) as co-catalyst, following analogous aluminum-based bicomponent systems that have recently succeeded in the efficient production of trisubstituted bicyclic terpene carbonates, including limonene carbonate **15** (see Figure S32 in the ESI†).[43]

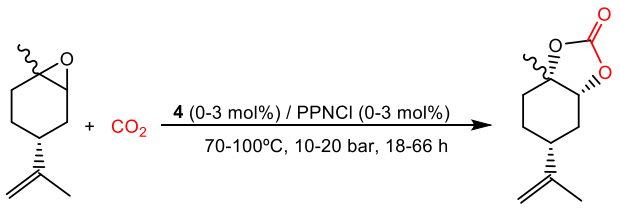

Scheme 5. Synthesis of cyclic carbonate **15** from (*R*)-(+)-limonene oxide using 1 mol% of complex **4** and 3 mol% PPNCl at 70 ºC and 10 bar CO_2 pressure for 66 hours

Table 4. Synthesis of (*R*)-(+)-limonene carbonate **15** catalyzed by **4** and PPNCl.

Entry	[4]/[PPNCl] (mol%)	*P*(CO_2) (bar)	T (ºC)	Time (h)	Conv. (%)[a]	Yield (%)[b] (*dr*, *trans*)
1	0.25:0.25	10	70	66	7	*nd*
2	3:3	10	70	18	27	22 (1:99)
3	1:3	10	70	18	21	16 (1:99)
4	1:3[c]	10	70	66	25	21 (1:99)
5	1:3	10	100	18	62	58 (6:94)
6	1:3	20	70	18	30	27 (1:99)
7	1:3	10	70	66	57	52 (1:99)
8	0:3	10	70	66	20	17 (>99)
9	1:3[d]	10	70	36	35	31
10	1:3[d]	10	70	66	79	76

[a] Determined by ^{1}H NMR spectroscopy of the crude reaction mixture. [b] Isolated yield after column chromatography. [c] TBAB as co-catalyst. [d] Experiment using only *trans*-limonene oxide.

We first assessed the synthesis of limonene carbonate **15** under the optimized reaction conditions for the synthesis of bio-based

This journal is © The Royal Society of Chemistry 20xx

Please do not adjust margins

Please do not adjust margins

derived cyclic carbonates **13c**–**13f** (70ºC, 10 bar CO_2, 18 h, 0.25 mol%). However, a rather low conversion was obtained even after 66 h of reaction (Table 4, entry 1), in accordance with the low reactivity of this trisubstituted epoxide **14**. Therefore, catalyst and co-catalyst loadings were increased up to 3 mol% in a 1:1 ratio,[43] and interestingly, 27% conversion was achieved after 18 h, while decreasing the concentration of complex **4** up to 1 mol% (1:3) did not produce significant change in catalytic activity (Table 4, entries 2–3). Expectedly, a control experiment using **4** and TBAB as co-catalyst (with larger halide, used for the synthesis of the cyclic carbonates **11a–j** and **13a**–**f**), resulted in considerably lower activity (Table 4, entry 4). Therefore, a combination of 1 mol% of **4** and 3 mol % of PPNCl was selected as the optimal loadings for this bicomponent catalytic system. Then, the effects of temperature, CO_2 pressure and reaction time were also investigated (Table 4, entries 5–7). As included in Table 4, an important loss of selectivity regarding the formation of cyclic carbonate **15** was detected when the reaction was carried out at 100 ºC due to the formation of several hydrolysis and rearrangement products, in agreement with analogous recent works.[41a] The increase of CO_2 pressure in two-folds (20 bar) did not produce significant growth on conversion, contrarily to the extension of time reaction (66 h). Consequently, we established as optimal reaction conditions for the selective production of the limonene carbonate **15** from epoxide **14**, 1:3 mol% of the bicomponent catalyst system **1**/PPNCl, 70 °C, and 10 bar of CO_2 pressure for 66 h (Table 4, entry 7). It is also worth noting that this reaction proceeded with high stereoselectivity to the *trans*-limonene carbonate in all cases. A control experiment using 3 mol % of PPNCl as catalyst reached only 20% conversion under identical conditions (Table 4, entry 8).

Once we optimized both the catalyst system and the reaction conditions for the synthesis of limonene carbonate **15**, we endeavoured the isolation of the *trans*-isomer of limonene oxide **14** from the commercially available *cis*/*trans* mixture, according to the literature procedure[44] (see Figure S31 in the ESI†), in order to increase the production of the *trans*-limonene carbonate **15** (see Scheme 5). We were pleased to find that the system **4**/PPNCl was very efficient and selective for the synthesis of the trisubstituted bicyclic *trans*-**15**, with complete stereochemical retention, reaching near 80% conversion at 70 °C and 10 bar CO_2 pressure in 66 hours using 1:3 mol% loading (Table 4, entries 9–10). For comparison with analogous bicomponent aluminum-based systems, catalyst **4** exhibited similar high efficiency for the *cis*/*trans* limonene oxide under milder conditions, using identical catalyst loading (*i.e*: 73% conv. for *trans*-**15**,[43] 85 ºC, 10 bar, 66 h, in MEK as solvent; 69% conv. for *cis*/*trans*-**15**,[21a] 80 ºC, 10 bar, 66 h; with M = La, 61% conv. for *cis*/*trans*-**15**,[45] 100 ºC, 10 bar, 66 h).

Conclusion

We have designed a novel family of bimetallic helical aluminum complexes of the type [AlR_2(κ^2-*NN*';κ^2-*NN*')AlR_2] via isolation of the preliminary adduct complexes or by direct heating of the protioligands with the alkylating agent. X-ray diffraction analysis confirmed the versatile coordination modes proposed for these ligands and the presence of helical chirality in the complexes. Based on DFT calculations, their preferential planar π-C_2N_2(sp^2)−Al_2 structure was justified and a plausible reaction mechanism proposed.

Bimetallics **2**–**3** and **4**–**9** in the presence of a co-catalyst resulted effective catalysts for CO_2 fixation into cyclic carbonates. The study led to the development of the bicomponent system **4**/(TBAB or PPNCl), which resulted very efficient and selective for the cycloaddition of CO_2 with a wide range of epoxides in good to excellent yields, and displayed really broad substrate scope, including internal and very challenging bio-based terpene derived substrates such as limonene oxide.

Although several one- and bicomponent aluminum-based catalysts have successfully proved to be very efficient for the cycloaddition of CO_2 and epoxides for cyclic carbonates production,[19,21,22] the development of more active and easily accessible dinuclear catalysts for the synthesis of cyclic carbonates from internal and biomass derived epoxides, still remains poorly explored.[21,22,42,43] We have developed an efficient Earth-abundant and inexpensive metal catalyst **4** that exhibits broader substrate scope, and presents excellent intramolecular cooperative catalytic features for internal and trisubstituted bio-based derived epoxides, giving near complete conversions under milder conditions.[21e,f,43,45] We consider these results firmly confirm a further step forward in our aim at developing more efficient catalysts for the sustainable fixation of CO_2 into cyclic carbonates.

Experimental Section

General Procedures

Reactions for the synthesis of complexes were performed using Schlenk techniques or a glovebox under an atmosphere of dry nitrogen. Solvents were predried over sodium wire and distilled under nitrogen from sodium (toluene and *n*-hexane) sodium-benzophenone (THF). Deuterated solvents were stored over activated 4 Å molecular sieves and degassed by several freeze-thaw cycles. The starting materials bis(3,5-dimethylpyrazole-1-yl)methane (bdmpzm), and the protioligands Hpbpamd, Htbpamd, Hphbpamd were prepared according to the literature procedures[24,28]. Butyllithium solution, $AlMe_3$, and $AlEt_3$ were used as purchased (Aldrich). (*R*)-Limonene oxide (*cis* and *trans* mixture) was distilled from calcium hydride under vacuum. The rest of the epoxide substrates were used as received unless specified otherwise (Aldrich, Across, Carbosynth). CO_2 (99,99%) was commercially obtained and used without further purification. All kinetics experiments were repeated at least twice and were mutually consistent.

Instruments and Measurements.

NMR spectra were recorded on a Varian Inova FT-400 spectrometer and were referenced to the residual deuterated solvent signal. The NOESY-1D spectra were recorded with the following acquisition parameters: irradiation time 2 s and number of scans 256 using standard VARIAN-FT software. 2D NMR spectra were acquired using the same software and processed using an IPC-Sun computer.

Preparation of Compounds 1–9.

Synthesis of [$AlMe_2$(κ^2-pbpamd)] (1). In a 100 mL Schlenk tube, Hpbpamd (1.00 g, 3.03 mmol) was dissolved in dry THF (25 mL) and cooled to -70 ºC. A solution of $AlMe_3$ (2.0 M in toluene) (1.51 mL, 3.03 mmol) was added and the mixture was allowed to warm up to 20 ºC and stirred during 6 hours. The solvent was removed *in vacuo* and

Please do not adjust margins

Please do not adjust margins

extracted with *n*-hexane (50 mL) and the resulting solution was concentrated *ca.* 10 mL and was cooled to -26 ºC to give compound **1** as a white semicrystalline solid. Yield 91%. Anal. Calcd. for $C_{20}H_{35}AlN_6$: C, 62.15; H, 9.13; N, 21.74 Found: C, 62.21; H, 9.19; N, 21.69. ^{1}H NMR (C_6D_6, 297 K), δ 5.63 s, 1 H, H^4), 5.23 (s, 1 H, H$^{4'}$), 5.21 (d, 1 H, $^3J_{H\text{-}H}$= 4 Hz, NH), 4.27 [sept, 1 H, $^3J_{H\text{-}H}$ = 8 Hz, NC*H*$(CH_3)_2$], 3.42 [sept, 1 H, $^3J_{H\text{-}H}$ = 8 Hz, NC*H*$(CH_3)_2$], 2.22 (s, 3 H, Me^5), 2.03 (s, 3 H, Me$^{5'}$), 1.70 (s, 3 H, Me^3), 1.53 (s, 3 H, Me$^{3'}$), 1.50 [d, 3 H, $^3J_{H\text{-}H}$= 8 Hz, NCH(C*H*$_3$)], 1.18 [d, 3 H, $^3J_{H\text{-}H}$= 8 Hz, NCH(C*H*$_3$)], 0.99 [d, 3 H, $^3J_{H\text{-}H}$= 8 Hz, NCH(C*H*$_3$)], 0.78 [d, 3 H, $^3J_{H\text{-}H}$= 8 Hz, NCH(C*H*$_3$)], -0.07 [s, 3 H, Al(C*H*$_3$)$_2$], -0.18 [s, 3 H, Al(C*H*$_3$)$_2$]. ^{13}C-{^{1}H} NMR (C_6D_6, 297 K), δ 152.5 (C^b), 147.8, 146.7, 142.7, 142.2 (C$^{3,3'\text{ or }5,5'}$), 107.3 (C^4), 105.1(C$^{4'}$), 97.5(C^a), 47.7, 46.5 [N*C*H$(CH_3)_2$], 25.8, 24.4, 23.7, 23.4 [NCH(*C*H$_3$)$_2$], 13.8 (Me^3), 13.0 (Me$^{3'}$), 11.1 (Me^5), 10.5 (Me$^{5'}$), -5.2, -8.1 [br, Al(*C*H$_3$)$_2$].

Synthesis of [AlMe$_2$(*κ*^{2}-pbpamd)AlMe$_3$] (2). In a 100 mL Schlenk tube, Hpbpamd (1.00 g, 3.03 mmol) was dissolved in dry THF (25 mL) and cooled to –70 ºC. A solution of $AlMe_3$ (2.0 M in toluene) (1.51 mL, 3.03 mmol) was added and the mixture was allowed to warm up to 20 ºC and stirred during 6 hours. The solvent was removed *in vacuo* and the product was dissolved in dry toluene (25 mL) and cooled to -70 ºC. A solution of $AlMe_3$ (2.0 M in toluene) (1.51 mL, 3.03 mmol) was added and the mixture was allowed to warm up to room temperature and stirred during 1 hour. The solvent was removed *in vacuo* and extracted with hexane (50 mL) and the resulting solution was concentrated *ca.* 10 mL and was cooled at –26 ºC to give compound **2** as a white semicrystalline solid. Yield: 82%. Anal. Calcd. for $C_{23}H_{44}Al_2N_6$: C, 60.24; H, 9.67; N, 18.33. Found: C, 60.29; H, 9.74; N, 18.38. ^{1}H NMR (C_6D_6, 297 K), δ 5.39 (s, 1 H, H^4), 5.25 (m, 1 H, NH), 5.14 (s, 1 H, H$^{4'}$), 4.25 [sept, 1 H, $^3J_{H\text{-}H}$ = 7.2 Hz, NC*H*$(CH_3)_2$], 3.46 [sept, 1 H, $^3J_{H\text{-}H}$ = 7.2 Hz, NC*H*$(CH_3)_2$] 2.25 (s, 3 H, Me^5), 1.98 (s, 3 H, Me$^{5'}$), 1.61 (s, 3 H, Me^3), 1.52 (s, 3 H, Me$^{3'}$), 1.47 [d, 3 H, $^3J_{H\text{-}H}$ = 7.2, NCH(C*H*$_3$)$_2$], 1.31 [d, 3 H, $^3J_{H\text{-}H}$ = 7.2, NCH(C*H*$_3$)$_2$], 1.02 [d, 3 H, $^3J_{H\text{-}H}$ = 7.2, NCH(C*H*$_3$)$_2$], 0.67 [d, 3 H, $^3J_{H\text{-}H}$ = 7.2, NCH(C*H*$_3$)$_2$], -0.12 [s, 3 H, Al(C*H*$_3$)], -0.17 [s, 9 H, Al*Me*$_3$], -0.28 [s, 3 H, Al(C*H*$_3$)].^{13}C-{^{1}H} NMR (C_6D_6, 297 K), δ 153.4 (C^b), 147.2, 146.7, 142.0, 141.9 (C$^{3,3'\text{ or }5,5'}$), 107.9 (C^4), 106.9 (C$^{4'}$), 98.1 (C^a), 48.3 [N*C*H$(CH_3)_2$], 46.8 [N*C*H$(CH_3)_2$], 26.2, 24.3, 24.2, 23.3 [NCH(*C*H$_3$)$_2$], 14.0 (Me^3), 13.0 (Me$^{3'}$), 11.7 (Me^5), 10.6 (Me$^{5'}$), -5.3 [br, Al(*C*H$_3$)$_2$], -5.9 [br, Al*Me*$_3$] -7.8 [br, Al(*C*H$_3$)$_2$].

Synthesis of [AlMe$_2$(*κ*^{2}-tbpamd)AlMe$_3$] (3). The synthesis of complex **3** was carried out in an identical manner to **2** using Htbpamd (1.00 g, 3.03 mmol) and $AlMe_3$ (2.0 M in toluene) (1.51 mL per equiv. added, 3.03 mmol per equiv. added). Yield: 85%. Anal. Calcd. for $C_{23}H_{44}AzI_2N_6$: C, 60.24; H, 9.67; N, 18.33. Found: C, 60.32; H, 9.71; N, 18.37. ^{1}H NMR (C_6D_6, 297 K), δ 5.29 (s, 1 H, H^4), 5.15 (s, 1 H, H$^{4'}$), 3.97 (q, 1 H, $^3J_{H\text{-}H}$ = 6.8 Hz, NC*H*$_2$CH$_3$) 3.64 (s, 1H, NH), 3.07 (q, 1 H, $^3J_{H\text{-}H}$ = 6.8 Hz, NC*H*$_2$CH$_3$), 2.25 (s, 3 H, Me^5), 1.97 (s, 3 H, Me$^{5'}$), 1.59 (s, 3 H, Me^3), 1.45 (s, 3 H, Me$^{3'}$), 1.24 (t, 3 H, $^3J_{H\text{-}H}$ = 6.8 Hz, NCH$_2$C*H*$_3$), 0.99 [s, 9 H, NC(C*H*$_3$)$_3$], -0.13 (s, 9 H, $AlMe_3$), -0.25 [s, 3 H, Al(C*H*$_3$)$_2$], -0.34 [s, 3 H, Al(C*H*$_3$)$_2$].^{13}C-{^{1}H} NMR (C_6D_6, 297 K), δ 152.3 (C^b), 146.7, 141.8 (C$^{3,3'\text{ or }5,5'}$), 108.1 (C^4), 107.7 (C$^{4'}$), 99.8 (C^a), 53.9 [N*C*$(CH_3)_3$], 42.7 (N*C*H$_2$CH$_3$), 30.6 [NC(*C*H$_3$)$_3$], 18.6 (NCH$_2$*C*H$_3$),14.1 (Me^3), 12.6 (Me$^{3'}$), 11.9 (Me^5), 10.8 (Me$^{5'}$), -5.2 [br, Al*Me*$_3$], -8.6 [br, Al(*C*H$_3$)$_2$], -8.4 [br, Al(*C*H$_3$)$_2$].

Synthesis of [AlMe$_2$(pbpamd$^-$)AlMe$_2$] (4). In a 100 mL Schlenk tube, Hpbpamd (1.00 g, 3.03 mmol) was dissolved in dry toluene (25 mL) and cooled to -70 ºC. A solution of $AlMe_3$ (2.0 M in toluene) (3.03 mL, 6.05 mmol) was added and the mixture was allowed to warm up to 70 ºC and stirred during 2 hours. The solvent was removed *in vacuo* and the product was precipited with hexane (40 mL). The compound was dissolved in dry toluene (25 mL) and the resulting solution was concentrated *ca.* 10 mL and was cooled at –26 ºC to give compound **4** as a white semicrystalline solid. Yield: 90% Anal. Calcd. for $C_{22}H_{40}Al_2N_6$: C, 59.71; H, 9.11; N, 18.99 Found: C, 59.85; H, 9.19; N, 18.78. ^{1}H NMR (C_6D_6, 297 K), δ 5.24 (s, 2 H, H$^{4,4'}$), 3.96 [sept, $^3J_{H\text{-}H}$ = 8 Hz, 2 H, NC*H*$(CH_3)_2$], 1.99 (s, 6 H, Me$^{5,5'}$), 1.51 [d, $^3J_{H\text{-}H}$ = 8 Hz, 6 H, NCH(C*H*$_3$)$_2$], 1.39 (s, 6 H, Me$^{3,3'}$), 1.03 [d, $^3J_{H\text{-}H}$ = 8 Hz, 6 H, NCH(C*H*$_3$)$_2$], -0.06 [s, 6 H, Al(C*H*$_3$)$_2$], -0.23 [s, 6 H, Al(C*H*$_3$)$_2$]). ^{13}C-{^{1}H} NMR (C_6D_6, 297 K), δ 160.6 (C^b), 146.7, 141.9 (C$^{3,3'\text{ or }5,5'}$), 106.7 (C$^{4,4'}$), 95.8 (C^a), 48.8 [N*C*H$(CH_3)_2$], 26.3, 24.1 [NCH(*C*H$_3$)$_2$], 12.9 (Me$^{3,3'}$), 9.9 (Me $^{5,5'}$), -5.9, -8.7 [br, Al(*C*H$_3$)$_2$].

Synthesis of [AlEt$_2$(pbpamd$^-$)AlEt$_2$] (5). The synthesis of complex **5** was carried out in an identical manner to **4** using Hpbpamd (1.00 g, 3.03 mmol) and $AlEt_3$ (1.0 M in toluene) (6.05 mL, 6.05 mmol). Yield: 88%. Anal. Calcd. for $C_{26}H_{48}Al_2N_6$: C, 62.62; H, 9.70; N, 16.85. Found: C, 62.68; H, 9.81; N, 16.75. ^{1}H NMR (C_6D_6, 297 K), δ 5.25 (s, 2 H, H$^{4,4'}$), 3.94 [sept, $^3J_{H\text{-}H}$ = 8 Hz, 2 H, NC*H*$(CH_3)_2$], 2.06 (s, 6 H, Me$^{5,5'}$),1.54 [t, $^3J_{H\text{-}H}$ = 8 Hz, 6 H, Al(CH$_2$C*H*$_3$)$_2$], 1.52 [d, $^3J_{H\text{-}H}$ = 6.8 Hz, 6 H, NCH(C*H*$_3$)$_2$], 1.47 [t, $^3J_{H\text{-}H}$ = 8 Hz, 6 H, Al(CH$_2$C*H*$_3$)$_2$], 1.34 (s, 6 H, Me$^{3,3'}$), 1.02 [d, $^3J_{H\text{-}H}$ = 6.8 Hz, 6 H, NCH(C*H*$_3$)$_2$], 0.55 [q, $^3J_{H\text{-}H}$ = 8 Hz, 4 H, Al(C*H*$_2$CH$_3$)$_2$], 0.33 [q, $^3J_{H\text{-}H}$ = 8 Hz, 4 H, Al(C*H*$_2$CH$_3$)$_2$]. ^{13}C-{^{1}H} NMR (C_6D_6, 297 K), δ 160.6 (C^b), 147.4, 142.1 (C$^{3,3'\text{ or }5,5'}$), 106.9 (C$^{4,4'}$), 95.8 (C^a), 48.7 [N*C*H$(CH_3)_2$], 26.3, 24.1 [NCH(*C*H$_3$)$_2$], 12.9 (Me$^{3,3'}$), 10.2 (Me $^{5,5'}$), 10.0, 9.9 [Al(CH$_2$*C*H$_3$)$_2$], 1.6, 0.3 [br, Al(*C*H$_2$CH$_3$)$_2$].

Synthesis of [AlMe$_2$(tbpamd$^-$)AlMe$_2$] (6). The synthesis of complex **6** was carried out in an identical manner to **4** but working at 90 ^{o}C and using Htbpamd (1.00 g, 3.03 mmol) and $AlMe_3$ (2.0 M in toluene) (3.03 mL, 6.05 mmol). Yield: 91%. Anal. Calcd. for $C_{22}H_{40}Al_2N_6$: C, 59.71; H, 9.11; N, 18.99. Found: C, 59.79; H, 9.18; N,18.92. ^{1}H NMR (C_6D_6, 297 K), δ 5.27 (s, 1 H, H^4), 5.22 (s, 1 H, H$^{4'}$), 3.92 (m, 1 H, NC*H*$_2$CH$_3$), 3.07 (m, 1 H, NC*H*$_2$CH$_3$), 2.00 (s, 3 H, Me^5), 1.97 (s, 3 H, Me$^{5'}$), 1.40 (s, 3 H, Me^3), 1.36 (s, 3 H, Me$^{3'}$), 1.32 [s, 9 H, NC(C*H*$_3$)$_3$], 1.09 [t, $^3J_{H\text{-}H}$ = 8 Hz, 3 H, NCH$_2$C*H*$_3$], 0.00 [s, 3 H, Al(C*H*$_3$)$_2$], -0.18 [s, 3 H, Al(C*H*$_3$)$_2$], -0.24 [s, 3 H, Al(C*H*$_3$)$_2$], -0.28 [s, 3 H, Al(C*H*$_3$)$_2$]. ^{13}C-{^{1}H} NMR (C_6D_6, 297 K), δ 152.4 (C^b), 151.8, 147.0, 146.8, 141.8 (C$^{3,3'\text{ or }5,5'}$), 108.2 (C^4), 107.9 (C$^{4'}$), 99.8 (C^a), 54.0 [N*C*$(CH_3)_3$], 42.7 (N*C*H$_2$CH$_3$), 30.7 [NC(*C*H$_3$)$_3$], 18.6 (NCH$_2$*C*H$_3$), 14.1 (Me^3), 12.6 (Me$^{3'}$), 12.0 (Me^5), 10.8 (Me$^{5'}$), -5.2, -8.6 [br, Al(*C*H$_3$)$_2$].

Synthesis of [AlEt$_2$(tbpamd$^-$)AlEt$_2$] (7). The synthesis of complex **7** was carried out in an identical manner to **6** using Htbpamd (1.00 g, 3.03 mmol) and $AlEt_3$ (1.0 M in toluene) (6.05 mL, 6.05 mmol). Yield: 87%. Anal. Calcd. for $C_{26}H_{48}Al_2N_6$: C, 62.62; H, 9.70; N, 16.84. Found: C, 62.69; H, 9.75; N, 16.79. ^{1}H NMR (C_6D_6, 297 K), δ 5.26 (s, 1 H, H^4), 5.24 (s, 1 H, H$^{4'}$), 3.85 (m, 1 H, NC*H*$_2$CH$_3$), 3.09 (m, 1 H, NC*H*$_2$CH$_3$), 2.06 (s, 3 H, Me^5), 2.02 (s, 3 H, Me$^{5'}$), 1.62 [t, $^3J_{H\text{-}H}$ = 8 Hz, 3 H, Al(CH$_2$C*H*$_3$)$_2$], 1.51 [m, 3 H, Al(CH$_2$C*H*$_3$)$_2$], 1.45 [m, 3 H, Al(CH$_2$C*H*$_3$)$_2$], 1.38 (s, 3 H, Me^3), 1.32 (s, 3 H, Me$^{3'}$), 1.30 [s, 9 H, NC(C*H*$_3$)$_3$], 1.09 [t, $^3J_{H\text{-}H}$ = 8 Hz, 3 H, NCH$_2$C*H*$_3$], 0.62 [m, 2 H, Al(C*H*$_2$CH$_3$)$_2$], 0.45 [m, 4 H, Al(C*H*$_2$CH$_3$)$_2$], 0.29 [m, 4 H, Al(C*H*$_2$CH$_3$)$_2$]. ^{13}C-{^{1}H} NMR (C_6D_6, 297 K), δ 158.1 (C^b), 147.5, 146.6, 142.9, 140.8 (C$^{3,3'\text{ or }5,5'}$), 107.1 (C^4), 106.3 (C$^{4'}$), 99.2 (C^a), 54.4 [N*C*$(CH_3)_3$], 42.3 (N*C*H$_2$CH$_3$), 32.4 [NC(*C*H$_3$)$_3$], 18.7 (NCH$_2$*C*H$_3$), 12.7 (Me$^{3,3'}$), 10.3 (Me$^{5,5'}$), 9.9, 9.8 [Al(CH$_2$*C*H$_3$)$_2$], 3.1, -0.1 [Al(*C*H$_2$CH$_3$)$_2$].

This journal is © The Royal Society of Chemistry 20xx

Please do not adjust margins

Please do not adjust margins

Synthesis of [AlMe$_2$(phbpamd$^-$)AlMe$_2$] (8). The synthesis of complex **8** was carried out in an identical manner to **4** but working at 50 ^{o}C and using Hphbpamd (1.00 g, 2.34 mmol) and AlMe$_3$ (2.0 M in toluene) (2.34 mL, 4.69 mmol). Yield: 92%. Anal. Calcd. for $C_{30}H_{40}Al_2N_6$: C, 66.89; H, 7.49; N, 15.60. Found: C, 66.95; H, 7.45; N, 15.67. ^{1}H NMR (C_6D_6, 297 K), δ 6.83 (d, $^3J_{H-H}$ = 8.12, 4 H, NC$_6$*H*$_4$Me), 6.77 (d, $^3J_{H-H}$ = 8.12, 4 H, NC$_6$*H*$_4$Me), 5.19 (s, 2 H, H$^{4,4'}$), 2.02 (s, 6 H, Me$^{5,5'}$), 1.92 (s, 6 H, NC$_6$H$_4$*Me*), 1.45 (s, 6 H, Me$^{3,3'}$), 0.08 [s, 6 H, Al(C*H*$_3$)$_2$], -0.37 [s, 6 H, Al(C*H*$_3$)$_2$]. ^{13}C-{^{1}H} NMR (C_6D_6, 297 K), δ 155.9 (C^b), 147.7, 144.7, 142.4, 130.5 (C$^{3,3'\text{ or }5,5'}$), 128.6-125.7 (N*C*$_6$H$_4$Me), 107.1 (C$^{4,4'}$), 95.6 (C^a), 20.8 (NC$_6$H$_4$*Me*), 12.7 (Me$^{3,3'}$), 10.0 (Me $^{5,5'}$), -9.2, -9.5 [br, Al(*C*H$_3$)$_2$].

Synthesis of [AlEt$_2$(phbpamd$^-$)AlEt$_2$] (9). The synthesis of complex **9** was carried out in an identical manner to **8** using Hphbpamd (1.00 g, 2.34 mmol) and AlEt$_3$ (1.0 M in toluene) (4.69 mL, 4.69 mmol). Yield: 89%. Anal. Calcd. for $C_{34}H_{48}Al_2N_6$: C, 68.66; H, 8.14; N, 14.13. Found: C, 68.73; H, 8.19; N, 14.17. ^{1}H NMR (C_6D_6, 297 K), δ 6.87 (d, $^3J_{H-H}$ = 8 Hz, 4 H, NC$_6$*H*$_4$Me), 6.80 (d, $^3J_{H-H}$ = 8 Hz, 4 H, NC$_6$*H*$_4$Me), 5.27 (s, 2 H, H$^{4,4'}$), 2.04 (s, 6 H, Me$^{5,5'}$), 1.64 [t, $^3J_{H-H}$ = 8 Hz, 6 H, Al(CH$_2$C*H*$_3$)$_2$], 1.41 04 (s, 6 H, Me$^{3,3'}$), 0.88 [t, $^3J_{H-H}$ = 8,4 Hz, 6 H, Al(CH$_2$C*H*$_3$)$_2$], 0.68 [q, $^3J_{H-H}$ = 8 Hz, 4 H, Al(C*H*$_2$CH$_3$)$_2$], 0.29 [q, $^3J_{H-H}$ = 8,4 Hz, 4 H, Al(C*H*$_2$CH$_3$)$_2$]. ^{13}C-{^{1}H} NMR (C_6D_6, 297 K), δ 156.2 (C^b), 148.4, 144.8, 142.7, 130.8 (C$^{3,3'\text{ or }5,5'}$), 129.3-125.8 (N*C*$_6$H$_4$Me), 107.0 (C$^{4,4'}$), 95.0 (C^a), 20.9 (NC$_6$H$_4$*Me*), 12.5 (Me$^{3,3'}$), 10.1 (Me $^{5,5'}$), 10.0, 8.6 [Al(CH$_2$*C*H$_3$)$_2$], 2.3, -0.3 [Al(*C*H$_2$CH$_3$)$_2$].

Acknowledgements

We gratefully acknowledge financial support from the Ministerio de Economía, y Competitividad (MINECO), Spain (Grant Nos. CTQ2017-84131-R, CTQ2016-78205-P and CTQ2016-81797-REDC Programa Redes Consolider).

Conflict of Interest

There are no conflicts to declare

Notes and references

1 J. Amouroux, P. Siffert, J. Pierre Massué, S. Cavadias, B. Trujillo, K. Hashimoto, P. Rutberg, S. Dresvin, X. Wang, *Prog. Nat. Sci-Mater*. 2014, **24**, 295-304; (b) W. E. Forum, 'Towards the Circular Economy: Accelerating the scale-up across global supply chains', can be found under: http://www3.weforum.org/docs/WEF_ENV_TowardsCircularEconomy_Report_2014.pdf, 2014.

2 M. Aresta, A. Dibenedetto, in *CO_2 Conversion and Utilization, Vol. 809*, American Chemical Society, 2002, pp. 54-70.

3 X.-Q. Zhang, C.-Z. Zhao, J.-Q. Huang, Q. Zhang, *Engineering* 2018, **4**, 831-847.

4 H. L. Parker, J. Sherwood, A. J. Hunt, J. H. Clark, *ACS Sustainable Chem. Eng.* 2014, **2**, 1739-1742.

5 M. A. Pacheco, C. L. Marshall, *Energy & Fuels* 1997, **11**, 2-29.

6 J. H. Clements, *Industrial & Engineering Chemistry Research* 2003, **42**, 663-674.

7 D. J. Darensbourg, *Chem. Rev.* 2007, **107**, 2388-2410.

8 Z. Han, L. Rong, J. Wu, L. Zhang, Z. Wang, K. Ding, *Angew. Chem. Int. Ed.* 2012, **51**, 13041-13045.

9 A. Duval, L. Avérous, *ACS Sustainable Chem. Eng.* 2017, **5**, 7334-7343.

10 A.-A. G. Shaikh, S. Sivaram, *Chem. Rev.* 1996, **96**, 951-976.

11 (a) W. Wang, Y. Wang, C. Li, L. Yan, M. Jiang, Y. Ding, *ACS Sustainable Chem. Eng.* 2017, **5**, 4523-4528; (b) V. D'Elia, H. Dong, A. J. Rossini, C. M. Widdifield, S. V. C. Vummaleti, Y. Minenkov, A. Poater, E. Abou-Hamad, J. D. A. Pelletier, L. Cavallo, L. Emsley, J.-M. Basset, *J. Am. Chem. Soc.* 2015, **137**, 7728-7739; (c) Z. Zhou, C. He, J. Xiu, L. Yang, C. Duan, *J. Am. Chem. Soc.* 2015, **137**, 15066-15069; (d) C. Kohrt, T. Werner, *ChemSusChem* 2015, **8**, 2031-2034; e) A. C. Kathalikkattil, R. Babu, J. Tharun, R. Roshan, D.-W. Park, *Catal. Surv. Asia* 2015, **19**, 223-235.

12 (a) R. R. Shaikh, S. Pornpraprom, V. D'Elia, *ACS Catalysis* 2018, **8**, 419-450; (b) H. Büttner, L. Longwitz, J. Steinbauer, C. Wulf, T. Werner, *Top. Curr. Chem.* 2017, **375**, 50; (c) C. Martín, G. Fiorani, A. W. Kleij, *ACS Catalysis* 2015, **5**, 1353-1370; (d) J. W. Comerford, I. D. V. Ingram, M. North, X. Wu, *Green Chem.* 2015, **17**, 1966-1987; (e) M. Cokoja, C. Bruckmeier, B. Rieger, W. A. Herrmann, F. E. Kühn, *Angew. Chem. Int. Ed.* 2011, **50**, 8510-8537.

13 (a) M. Alves, B. Grignard, R. Mereau, C. Jerome, T. Tassaing, C. Detrembleur, *Catal. Sci. Technol.* 2017, **7**, 2651-2684; (b) G. Fiorani, W. Guo, A. W. Kleij, *Green Chem.* 2015, **17**, 1375-1389.

14 (a) K. Ni, C. M. Kozak, *Inorg. Chem.* 2018, **57**, 3097-3106; (b) K. Devaine-Pressing, L. N. Dawe, C. M. Kozak, *Polym. Chem.* **2015**, *6*, 6305-6315; (c) D. J. Darensbourg, R. R. Poland, A. L. Strickland, *J. Polym. Sci., Part A: Polym. Chem.* 2012, **50**, 127-133.

15 (a) X. Jiang, F. Gou, F. Chen, H. Jing, *Green Chem.* 2016, **18**, 3567-3576; (b) X.-B. Lu, D. J. Darensbourg, *Chem. Soc. Rev.* 2012, **41**, 1462-1484; (c) A. Sibaouih, P. Ryan, M. Leskelä, B. Rieger, T. Repo, *Appl. Catal. A-Gen.* 2009, **365**, 194-198.

16 (a) F. Della Monica, A. Buonerba, C. Capacchione, *Adv. Synth. Catal.* 2019, **361**, 265-282; (b) E. Y. Seong, J. H. Kim, N. H. Kim, K.-H. Ahn, E. J. Kang, *ChemSusChem* 2019, **12**, 409-415; (c) F. Chen, N. Liu, B. Dai, *ACS Sustainable Chem. Eng.* 2017, **5**, 9065-9075.

17 (a) C. Maeda, T. Taniguchi, K. Ogawa, T. Ema, *Angew. Chem. Int. Ed.* 2015, **54**, 134-138; (b) T. Ema, Y. Miyazaki, J. Shimonishi, C. Maeda, J.-Y. Hasegawa, *J. Am. Chem. Soc.* 2014, **136**, 15270-15279; (c) T. Ema, Y. Miyazaki, S. Koyama, Y. Yano, T. Sakai, *Chem. Commun.* 2012, **48**, 4489-4491.

18 (a) S. Sobrino, M. Navarro, J. Fernández-Baeza, L. F. Sánchez-Barba, A. Garcés, A. Lara-Sánchez, J. A. Castro-Osma, *Dalton Trans.* 2019, **48**, 10733-10742; (b) X.-D. Lang, Y.-C. Yu, L.-N. He, *J. Mol. Catal. A: Chem.* 2016, **420**, 208-215; (c) C. Maeda, J. Shimonishi, R. Miyazaki, J.-y. Hasegawa, T. Ema, *Chem. Eur. J.* 2016, **22**, 6556-6563; (d) M. A. Fuchs, S. Staudt, C. Altesleben, O. Walter, T. A. Zevaco, E. Dinjus, *Dalton Trans.* 2014, **43**, 2344-2347; (e) R. Luo, X. Zhou, S. Chen, Y. Li, L. Zhou, H. Ji, *Green Chem.* 2014, **16**, 1496-1506; (f) Y. Yang, Y. Hayashi, Y. Fujii, T. Nagano, Y. Kita, T. Ohshima, J. Okuda, K. Mashima, *Catal. Sci. Technol.* 2012, **2**, 509-513.

19 (a) Y. Kim, K. Hyun, D. Ahn, R. Kim, M. H. Park, Y. Kim, *ChemSusChem* 2019, **12**, 4211-4220; (b) J. Rintjema, A. W. Kleij, *ChemSusChem* 2017, **10**, 1274-1282; (c) M. Cozzolino, T. Rosen, I. Goldberg, M. Mazzeo, M. Lamberti, *ChemSusChem* 2017, **10**, 1217-1223; (d) J. Rintjema, R. Epping, G. Fiorani, E. Martín, E. C. Escudero-Adán, A. W. Kleij, *Angew. Chem. Int. Ed.* 2016, **55**, 3972-3976; (e) S. H. Kim, D. Ahn, M. J. Go, M. H. Park, M. Kim, J. Lee, Y. Kim, *Organometallics* 2014, **33**, 2770-2775; (f) R. Luo, X. Zhou, S. Chen, Y. Li, L. Zhou, H. Ji, *Green Chem.* 2014, **16**, 1496-1506; (g) J. Meléndez, M. North, P. Villuendas, C. Young, *Dalton Trans.* 2011, **40**, 3885-3902; (h) M. North, C. Young, *Catal. Sci. Technol.* 2011, **1**, 93-99.

Please do not adjust margins

Please do not adjust margins

20 A. Otero, J. Fernández-Baeza, A. Lara-Sánchez, L. F. Sánchez-Barba, *Coord. Chem. Rev.* 2013, **257**, 1806-1868.

21 (a) F. de la Cruz-Martínez, M. Martínez de Sarasa Buchaca, J. Martínez, J. Fernández-Baeza, L. F. Sánchez-Barba, A. Rodríguez-Diéguez, J. A. Castro-Osma, A. Lara-Sánchez, *ACS Sustainable Chem. Eng.* 2019, **7**, 20126-20138; (b) M. A. Gaona, F. de la Cruz-Martínez, J. Fernández-Baeza, L. F. Sánchez-Barba, C. Alonso-Moreno, A. M. Rodríguez, A. Rodríguez-Diéguez, J. A. Castro-Osma, A. Otero, A. Lara-Sánchez, *Dalton Trans.* 2019, **48**, 4218-4227; (c) J. Martínez, F. de la Cruz-Martínez, M. A. Gaona, E. Pinilla-Peñalver, J. Fernández-Baeza, A. M. Rodríguez, J. A. Castro-Osma, A. Otero, A. Lara-Sánchez, *Inorg. Chem.* 2019, **58**, 3396-3408; (d) F. de la Cruz-Martínez, J. Martínez, M. A. Gaona, J. Fernández-Baeza, L. F. Sánchez-Barba, A. M. Rodríguez, J. A. Castro-Osma, A. Otero, A. Lara-Sánchez, *ACS Sustainable Chem. Eng.* 2018, **6**, 5322-5332; (e) J. Martínez, J. A. Castro-Osma, C. Alonso-Moreno, A. Rodríguez-Diéguez, M. North, A. Otero, A. Lara-Sánchez, *ChemSusChem* 2017, **10**, 1175-1185; (f) J. Martínez, J. A. Castro-Osma, A. Earlam, C. Alonso-Moreno, A. Otero, A. Lara-Sánchez, M. North, A. Rodríguez-Diéguez, *Chem. Eur. J.* 2015, **21**, 9850-9862; (g) J. A. Castro-Osma, C. Alonso-Moreno, A. Lara-Sánchez, J. Martínez, M. North, A. Otero, *Catal. Sci. Technol.* 2014, **4**, 1674-1684.

22 (a) D. O. Meléndez, A. Lara-Sánchez, J. Martínez, X. Wu, A. Otero, J. A. Castro-Osma, M. North, R. S. Rojas, *ChemCatChem* 2018, **10**, 2271-2277; (b) X. Wu, M. North, *ChemSusChem* 2017, **10**, 74-78; (c) W. Clegg, R. W. Harrington, M. North, R. Pasquale, *Chem. Eur. J.* 2010, **16**, 6828-6843; (d) M. North, R. Pasquale, *Angew. Chem. Int. Ed.* 2009, **48**, 2946-2948; (e) J. Meléndez, M. North, R. Pasquale, *Eur. J. Inorg. Chem.* 2007, 3323-3326.

23 A. Garcés, L. F. Sánchez-Barba, J. Fernández-Baeza, A. Otero, I. Fernández, A. Lara-Sánchez, A. M. Rodríguez, *Inorg. Chem.* 2018, **57**, 12132-12142.

24 (a) J. A. Castro-Osma, C. Alonso-Moreno, M. V. Gómez, I. Márquez-Segovia, A. Otero, A. Lara-Sánchez, J. Fernández-Baeza, L. F. Sánchez-Barba, A. M. Rodríguez, *Dalton Trans*., 2013, **42**, 14240-14252; (b) A. Otero, A. Lara-Sánchez, J. Fernández-Baeza, C. Alonso-Moreno, J. Tejeda, J. A. Castro-Osma, I. Márquez-Segovia, L. F. Sánchez-Barba, A. M. Rodríguez and M. V. Gómez, *Chem. Eur. J*. 2010, **16**, 8615-8619.

25 (a) L. Wang, C. Xu, Q. Han, X. Tang, P. Zhou, R. Zhang, G. Gao, B. Xu, W. Qin, W. Liu, *Chem. Commun*., 2018, **54**, 2212-2215; (b) A. P. Paneerselvam, S. S. Mishra, D. K. Chand *J. Chem. Sci.*, 2018, 130:96.

26 (a) M. A. Gaona, F. de la Cruz-Martínez, J. Fernández-Baeza, L. F. Sánchez-Barba, C. Alonso-Moreno, A. M. Rodríguez, A. Rodríguez-Diéguez, J. A. Castro-Osma, A. Otero, A. Lara-Sánchez *Dalton Trans*., 2019, **48**, 4218–4227; (b) J. Martínez, M. Martínez de Sarasa Buchaca, F. de la Cruz-Martínez, C. Alonso-Moreno, L. F. Sánchez-Barba, J. Fernandez-Baeza, A. M. Rodríguez, A. Rodríguez-Diéguez, J. A. Castro-Osma, A. Otero and A. Lara-Sánchez, *Dalton Trans*., 2018, **47**, 7471-7479.

27 C. Alonso-Moreno, A. Garcés, L. F. Sánchez-Barba, M. Fajardo, J. Fernández-Baeza, A. Otero, A. Lara-Sánchez, A. Antiñolo, L. Broomfield, M. I. López-Solera, A. M. Rodríguez, *Organometallics* 2008, **27**, 1310-1321.

28 A. Garcés, L. F. Sánchez-Barba, J. Fernández-Baeza, A. Otero, A. Lara-Sánchez, A. M. Rodríguez, *Organometallics* 2017, **36**, 884-897.

29 (a) H. A. Favre, W. H. Powell, 'International Union of, P.; Applied, C. Nomenclature of Organic Chemistry: IUPAC Recommendations and Preferred Names 2013' can be found under, http://public.eblib.com/choice/publicfullrecord.aspx?p=1713731, 2013; (b) J. A. Castro-Osma, C. Alonso-Moreno, M. V. Gómez, I. Márquez-Segovia, A. Otero, A. Lara-Sánchez, J. Fernández-Baeza, L. F. Sánchez-Barba, A. M. Rodríguez, *Dalton Trans.* 2013, **42**, 14240-14252.

30 J. A. Castro-Osma, C. Alonso-Moreno, A. Lara-Sánchez, A. Otero, J. Fernández-Baeza, L. F. Sánchez-Barba, A. M. Rodríguez, *Dalton Trans.* 2015, **44**, 12388-12400.

31 (a) V. D'Elia, A. A. Ghani, A. Monassier, J. Sofack-Kreutzer, J. D. A. Pelletier, M. Drees, S. V. C. Vummaleti, A. Poater, L. Cavallo, M. Cokoja, J.-M. Basset, F. E. Kühn, *Chem. Eur. J.* 2014, **20**, 11870-11882; (b) D. R. Moore, M. Cheng, E. B. Lobkovsky, G. W. Coates, *J. Am. Chem. Soc.* 2003, **125**, 11911-11924.

32 R. Babu, A. C. Kathalikkattil, R. Roshan, J. Tharun, D.-W. Kim, D.-W. Park, *Green Chem.* 2016, **18**, 232-242.

33 H. Kawanami, A. Sasaki, K. Matsui, Y. Ikushima, *Chem. Commun.* 2003, 896-897.

34 (a) C. J. Whiteoak, E. Martin, M. M. Belmonte, J. Benet-Buchholz, A. W. Kleij, *Adv. Synth. Catal.* 2012, **354**, 469-476; (b) D. J. Darensbourg, A. Horn Jr, A. I. Moncada, *Green Chem.* 2010, **12**, 1376-1379.

35 (a) R. Ma, H. Sun, Y. Cui, *RSC Adv.* 2018, **8**, 11145-11149; (b) P. Gao, Z. Zhao, L. Chen, D. Yuan, Y. Yao, *Organometallics* 2016, **35**, 1707-1712; (c) C. J. Whiteoak, N. Kielland, V. Laserna, E. C. Escudero-Adán, E. Martin, A. W. Kleij, *J. Am. Chem. Soc.* 2013, **135**, 1228-1231.

36 C. Beattie, M. North, P. Villuendas, C. Young, *J. Org. Chem.* 2013, **78**, 419-426.

37 (a) J. Peng, S. Wang, H.-J. Yang, B. Ban, Z. Wei, L. Wang, L. Bo, *Catal. Today* 2019, **330**, 76-84; (b) Y. Ren, J. Chen, C. Qi, H. Jiang, *ChemCatChem* 2015, **7**, 1535-1538; (c) S. I. Vagin, R. Reichardt, S. Klaus, B. Rieger, *J. Am. Chem. Soc.* 2010, **132**, 14367-14369; (d) J. Meléndez, M. North, P. Villuendas, *Chem. Commun.* 2009, 2577-2579.

38 (a) J. Datta, M. Włoch, *Polym. Bull.* 2016, **73**, 1459-1496; (b) G. Rokicki, P. G. Parzuchowski, M. Mazurek, *Polym. Adv. Technol.* 2015, **26**, 707-761.

39 F. Hu, J. J. La Scala, J. M. Sadler, G. R. Palmese, *Macromolecules* 2014, **47**, 3332-3342.

40 L. Annunziata, S. Fouquay, G. Michaud, F. Simon, S. M. Guillaume, J.-F. Carpentier, *Polym. Chem.* **2013**, *4*, 1313-1316.

41 (a) K. A. Maltby, M. Hutchby, P. Plucinski, M. G. Davidson, U. Hintermair, *Chem. Eur. J.* 2020, doi.org/10.1002/chem.201905561. (b) M. Firdaus, L. Montero de Espinosa, M. A. R. Meier, *Macromolecules* 2011, **44**, 7253-7262.

42 A. Rehman, A. M. López Fernández, M. F. M. Gunam Resul, A. Harvey, *J. CO2 Util.* 2019, **29**, 126-133.

43 G. Fiorani, M. Stuck, C. Martín, M. M. Belmonte, E. Martin, E. C. Escudero-Adán, A. W. Kleij, *ChemSusChem* 2016, **9**, 1304-1311.

44 D. Steiner, L. Ivison, C. T. Goralski, R. B. Appell, J. R. Gojkovic, B. Singaram, *Tetrahedron: Asymmetry* 2002, **13**, 2359-2363.

45 J. Martínez, J Fernández-Baeza, L. F. Sánchez-Barba, J. A. Castro-Osma, A. Lara-Sánchez, A. Otero *ChemSusChem* 2017, **10**, 2886-2890.

This journal is © The Royal Society of Chemistry 20xx

Please do not adjust margins

Please do not adjust margins

Entry for the Table of Contents

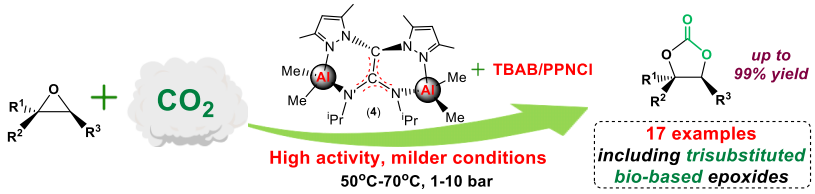

The reaction of scorpionate ligands with 2 equiv of AlR_3 proceed easily to give bimetallic helical aluminum complexes [AlR_2(κ^2-*NN*';κ^2-*NN*')AlR_2]. Importantly, the combination of dinuclear **4** and TBAB/PPNCl behaves as an excellent and selective bicomponent system for cyclic carbonate formation from CO_2 with a very broad range of challenging epoxides, including internal and bio-based trisubstituted terpene derived as limonene oxide.

This journal is © The Royal Society of Chemistry 20xx

Please do not adjust margins